Optical study of 2D photonic crystals in an InP/GaInAsP slab waveguide structure

Rolando Ferrini[1], David Leuenberger[1], Mikaël Mulot[2], Min Qiu[2], Jürgen Moosburger[3], Martin Kamp[3], Alfred Forchel[3], Srinivasan Anand[2], and Romuald Houdré[1]
[1]Institut de Micro et Opto-électronique, Ecole Polytechnique Fédérale de Lausanne, CH-1015 Lausanne, Switzerland.
[2]Department of Microelectronics and Information Technology, Royal Institute of Technology , Electrum 229, S-16440 Kista, Sweden.
[3]Technische Physik, University of Würzburg, Am Hubland, D-97074 Würzburg, Germany.

ABSTRACT

We report on the optical properties of two dimensional (2D) photonic crystals (PCs) deeply etched in an InP/GaInAsP step-index waveguide. Transmission (T) measurements through simple PC slabs and through one-dimensional (1D) Fabry-Pérot (FP) cavities between PC mirrors are reported and compared to theory. A 2D finite difference time-domain (FDTD) method combined to a phenomenological out-of-plane loss model is used to assess different loss contributions. The PC optical properties are deduced from the FP peak analysis. The origin of the high T level observed inside the stopgap is investigated.

INTRODUCTION

In photonic crystal (PC) structures the periodic arrangement of different elements with strong dielectric contrast affects the properties of photons forbidding light propagation along specific directions within relatively large energy bands known as *photonic band-gaps* (PBGs) [1,2]. In the last few years it has been proved that, although an omnidirectional PBG is only possible in a three-dimensional (3D) PC, a two-dimensional (2D) PC combined to a vertical step-index waveguide offers enough light control for integrated optics applications [3]. The potentials of this approach have been successfully demonstrated both in GaAs-based structures ($\lambda \approx 1.0$ μm) [3] and in InP-based systems at telecommunication application wavelengths ($\lambda \approx 1.5$ μm) [4]. In this paper we describe the optical characterization of *quasi*-2D PCs deeply etched into an InP/GaInAsP slab waveguide. The internal light source (ILS) technique is used to measure the transmission (T) spectra through simple PC slabs and one-dimensional (1D) Fabry-Pérot (FP) cavities formed between two PC mirrors. A 2D finite difference time-domain (FDTD) method is used to best fit the experimental data. The exact amount of out-of-plane losses is assessed and the hole depth/shape contributions are analyzed. The optical properties of the PC structures are determined and the origin of the high T level detected inside the stopgap is discussed.

EXPERIMENT

Quasi-2D PCs consisting of a triangular lattice of air holes were fabricated on nominally undoped GaInAsP/InP heterostructures grown by metal organic vapor phase epitaxy (MOVPE) on *n*-InP substrates (see figure 1(a)). Moderate filling factor values ($f \approx 0.30$) were chosen in order to minimize out-of-plane losses [3,4]. Such low f values result in a full gap only in the

transverse electric (TE) polarization direction. The PC structures were etched normally to an InP/GaInAsP/InP slab waveguide containing a built-in light source. The waveguide core is a 434 nm-thick $Ga_{0.24}In_{0.76}As_{0.52}P_{0.48}$ layer lattice matched to InP and sandwiched between a 200 nm-thick InP cap layer and a 600 nm-thick InP buffer layer. In the spectral region of interest (*i.e.*, $\lambda \approx 1550$ nm) the values $n_{core} = 3.35$ and $n_{clad} = 3.17$ are assumed for the refraction index of GaInAsP and InP, respectively. The resulting structure is a multimode waveguide with a fundamental guided TE mode corresponding to an effective index $n_{eff} = 3.24$ [4]. The light source consists of two different GaInAsP strain-compensated quantum well (QW) packages separated by a 30 nm spacer and located approximately in the middle of the guiding structure between two 181 nm-thick barrier layers. Due to the superimposition of the two QW signals ($\lambda_1 = 1.47$ μm and $\lambda_2 = 1.55$ μm) a 100 nm-wide PL peak centered at 1500 nm is obtained [4].

Electron beam (e-beam) lithography was used to define the PC patterns, while dry etching techniques were applied to transfer the pattern into the semiconductor heterostructure. In order to form a durable SiO_2 etch mask for the subsequent etch process the procedure described in [4,5] was adopted. Ar/Cl_2 chemically assisted ion beam etching (CAIBE) [4] and Cl_2/Ar-based electron cyclotron resonance-RIE (ECR-RIE) [5] were used to pattern sample #1 and sample #2, respectively. As sketched in figure 1(a), the obtained hole shape is conical with nearly vertical walls close to the surface and a strongly tapered bottom. Figures 1(b) and (c) show the cross-section view scanning electron microscopy (SEM) micrographs of two PC test structures for sample #1 and sample #2, respectively. In sample #1 the holes have oblique walls already inside the waveguide core (z_2) and a slight bending towards the hole bottom is observed. Nevertheless, the hole pattern is "ordered": no dispersion in the hole depth $z = z_2 + \Delta z$ is found when the hole diameter (D) is kept constant. z values of 2.55 μm are obtained for the larger holes [4]. On the contrary, in sample #2 fluctuations appear in the hole depth yielding $\langle z \rangle \geq 3$ μm, while no bending is present and the holes have straight walls inside z_2.

The ILS technique described in [4] was used to characterize the PC optical properties.

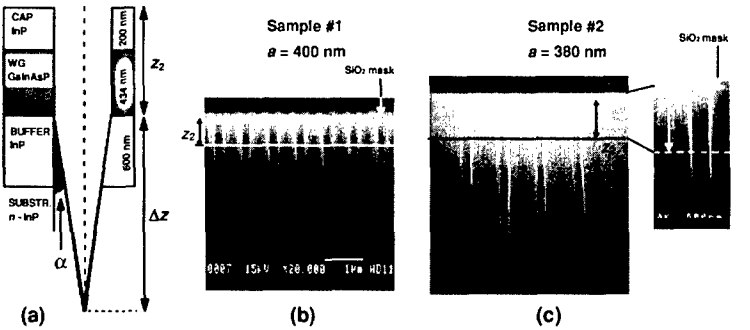

Figure 1. (a) Sketch of the InP/GaInAsP waveguide (WG) heterostructure. The hole shape model used to calculate the loss parameter value ε" is illustrated. z_2 is the thickness of the cap + WG layer where the holes are assumed to be cylindrical, while Δz is the cone depth. The cone half angle α is also evidenced. (b) and (c): edge view SEM micrographs of test photonic crystal (PC) structures for sample #1 and sample #2, respectively. The images were taken before the removal of the SiO_2 mask. In the inset of figure (c) the cylindrical shape of sample #2 holes inside z_2 is evidenced.

The PL excited inside the GaInAsP QWs is used as a built-in probe beam. Part of the PL signal propagates parallel to the surface as a guided mode and interacts with the PC structure. The absolute PC T spectrum is obtained normalizing the spectrum detected after transmission through the PC structure with respect to the spectrum collected in a non-patterned region of the sample. Details on the experimental set-up and on the measurement schemes adopted for simple PC slabs and 1D FP cavities are given in [4]. Here we remind that, since ILS measurements on a single PC structure yield the T spectrum only in a narrow interval (≈ 100 nm), the "lithographic tuning" approach has to be applied in order to determine the PC optical properties within a wide spectral range. As the QW emission wavelength is fixed, the scaling property of PCs [1] is used and PC structures with different periods a are measured. If f is kept constant the whole PBG can be explored as a function of the reduced frequency $u = a / \lambda$ [3,4].

RESULTS AND DISCUSSION

T spectra through PC slabs along both ΓM and ΓK orientations and for TE polarization are shown in figures 2 (a) and (b) for sample #1 (10 rows thick slab) and #2 (8 rows), respectively. The layout of simple PC slabs is shown in figure 2 (c). Both ΓM and ΓK oriented structures were fabricated with periods a ranging from 240 to 500 nm for sample #1 (Δa = 20 nm) and from 240 to 640 nm for sample #2 (Δa = 20 nm). Well-defined PBGs appear in each spectrum with steep dielectric band edges at u = 0.19 and 0.22 for ΓM and ΓK orientations, respectively. On the other hand, due to the strong influence of out-of-plane losses on T at the air band edge [3], smooth T bands appear at $u \approx 0.28$ and 0.30 for ΓM and ΓK orientations, respectively. T values between 80% and 90% are reached for $u < 0.20$, while T ≤ 40% for $u \geq 0.30$. Finally, an average T ≈ 3 – 5% is observed inside the PBG for both samples.

The experimental T spectra are compared to theoretical spectra calculated with a 2D FDTD model [6]. The effect of the vertical confinement on the light propagating through the PC slabs

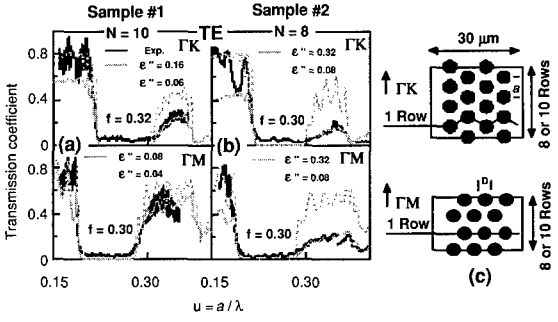

Figure 2. TE transmission spectra through ΓM and ΓK oriented photonic crystal (PC) slabs for (a) sample #1 (10 rows) and (b) sample #2 (8 rows), respectively. Experimental spectra (black lines) are compared with 2D finite difference time-domain (FDTD) calculated spectra (gray lines). (c) Sketch of the typical layout of simple PC structures along ΓM and ΓK orientations. Each slab is characterized by the period a (or hole diameter D) value. Hairlines show the single "atomic" plane for both orientations.

was taken into account assuming $n \equiv n_{eff} = 3.24$ for the dielectric matrix. Out-of-plane losses were cast into the 2D calculation by introducing the imaginary ε" as a phenomenological loss parameter [4,7]. f and ε" were chosen as free parameters of the fit. The best-fitted curves are reported in figures 2(a) and (b), while in table I the obtained f and ε" values are listed. While for sample #2 both ΓM and ΓK spectra are fitted assuming the same f value, for sample #1 f (ΓK) > f (ΓM). The latter discrepancy is due to the hole squeezing along the ΓK direction originating in the e-beam lithography of sample #1 [4]. Different ε" values have to be used to fit either the dielectric or the air T band edge in both samples. As shown in [4], $\varepsilon'' \propto (u^2 \times f)$: if f is constant while increasing u, higher ε" values have to be introduced. Moreover, when u is fixed, f (ΓK) > f (ΓM) implies ε" (ΓK) > ε" (ΓM). Finally, the sample #2 ε" values are always higher than the corresponding values of sample #1. The different out-of-plane loss level in the two samples has to be ascribed to differences in the hole morphology and in the PC pattern disorder (see below).

The ε" values obtained from the best fit of the air band edge were analyzed in the framework of a loss model where the total loss parameter is expressed as $\varepsilon'' = \varepsilon''_{int} + \varepsilon''_{hole}$ [8,9]. ε''_{hole} contains contributions from the finite etch depth and from the conical hole shape, while ε''_{int} accounts for the intrinsic losses corresponding to the ideal case of infinitely deep holes. Since for these InP-based PC structures $\varepsilon''_{int} = 0.01 - 0.02$ [4], the values ε''_{hole} (#1) = 0.105 ± 0.045 and ε''_{hole} (#2) = 0.305 ± 0.005 derive for sample #1 and #2, respectively. Following the procedure illustrated in [9] and adopting the model hole shape sketched in figure 1(a), the theoretical value ε''_{hole} can be calculated. If the exponential decaying field profile $\zeta(z) = A \exp(Kz)$ is assumed in the substrate, ε''_{hole} is a function of K and of the cone slope α in the first $L_{decay} = K^{-1}$ [9]. From the SEM micrograph analysis $\alpha \approx 2.5° \pm 0.5°$ for both samples and $\varepsilon''_{hole} \approx 0.30$ is obtained. While the latter value perfectly agrees with ε''_{hole} (#2), it is 2 – 4 times higher than ε''_{hole} (#1). As mentioned in [4], the discrepancy between the calculated and the experimental ε''_{hole} (#1) values originates from the complex hole geometrical shape (*e.g.*, hole bending, oblique walls inside the core) which does not fit the assumed model shape. On the contrary, when holes keep straight walls inside the cap + waveguide layer (z_2), the different loss contributions can be deduced from the ε" experimental values and ε''_{hole} can be easily modeled. Extrapolating from sample #2 data, two perspectives emerge which can be considered realistic for the actual etching techniques. First, it is found that the minimum loss limit ε''_{int} could be reached for $\alpha \leq 0.5°$, *i.e.* for holes with almost straight walls in some L_{decay}'s inside the substrate. On the other hand, a less critical reduction in the cone slope would make possible to get a sufficiently low loss level for good performance PC applications (*e.g.*, $\varepsilon'' \leq 0.1$ for $\alpha \leq 1.5°$) [8].

In order to investigate the PC optical properties inside the PBG, 1D FP cavities were fabricated for both samples using 4 rows thick ΓM-oriented PC-based mirrors (a = 300 - 480 nm

Table I. Photonic crystal (PC) slabs : f and ε" values (FDTD fit). 1D Fabry-Pérot (FP) cavities : optical properties of a single 4 row PC mirror and cavity parameter values (Airy's function fit).

Sample	PC slabs - FDTD fit					1D - FP Cavities - Airy's function fit					
	N		f	ε" (Diel. B.)	ε" (Air B.)	T (%)	R (%)	L (%)	L_p/a	m	Q
#1	10	ΓM	0.30	0.04	0.08	a = 340 nm ; W/a = 1.9					
		ΓK	0.32	0.06	0.16	14	64	22	0.36	4	28
#2	8	ΓM	0.30	0.08	0.32	a = 340 nm ; W/a = 2.0					
		ΓK	0.30	0.08	0.32	10	80	10	0.40	4	56

and Δa = 20 nm) separated by a spacer with a normalized width W / a = 1.7 - 2.2 [4]. A typical T spectrum through a 1D FP cavity is shown in figure 3(a) for sample #2 (W / a = 2.0). The cavity layout is sketched in figure 3(b). The two peaks appearing in the T spectrum at u = 0.22 and u = 0.29 are due to first and second-order FP resonances, respectively. The experimental spectrum is compared to the calculated 2D-FDTD T spectrum. The ΓM values derived from the best fit of simple PC slab air band edges were adopted for f and ε", while the value W / a = 1.97 was assumed for the cavity width. As for simple PC slabs, FDTD calculated spectra do not agree with the experimental data inside the PBG: the theoretical T value inside the gap ($T \approx 10^{-2} - 10^{-4}$ %) is higher than the detected value (T ≈ 3 – 5 %). While the experimental FP peaks are located at energies consistent with the calculated values, they show higher peak T and lower quality factors Q than the simulated peaks. As shown in the inset of figure 3(a) the Airy's formula for planar resonators is used to fit the first-order FP resonances [4] yielding the optical properties of a single 4 row PC mirror (see table I).

The comparison between the separate analysis of simple PC slab and 1D FP cavity spectra for both samples completes the picture given in [4]. While the fit of the T air band edges yields ε"(#2) > ε"(#1), from the best fit of FP resonances inside the PBG the total loss value L (#2) is found to be lower than the corresponding L (#1) value. Moreover, in sample #2 the T level inside the stopgap decreases while reflectivity (R) increases to 80% giving Q (#2) ≈ 2 × Q (#1). In order to explain this apparent discrepancy we remind that two different effects may affect light propagation through a PC structure [4]. First, the finite hole depth contributes to increase out-of-plane scattering. On the other hand, when entering the PC, the hole pattern is felt as a low refractive index contrast region and light is pushed below the guiding layer (*modal conversion*). When energies outside the stopgap are considered, light propagation is allowed and Bloch modes propagate into the PC. As pointed out in [10], Bloch modes are strongly influenced by defects and/or disorder where out-of-plane scattering can occur. Therefore, due to dispersion in the cone depth Δz (see figure 1(c)) which contributes to disorder, out-of-plane losses are found to be higher in sample #2 than in sample #1. On the contrary, the second effect becomes predominant inside the stopgap. Light propagation is forbidden and "evanescent" modes penetrate the PC.

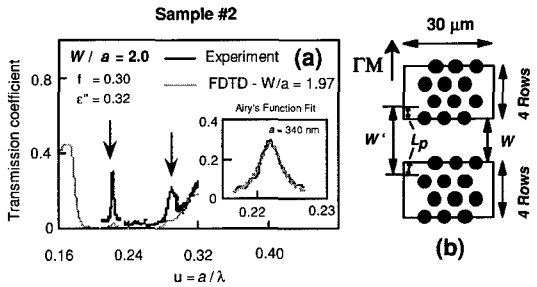

Figure 3. (a) Transmission spectrum through a 1D Fabry-Pérot (FP) cavity between two ΓM oriented 4 rows photonic crystal (PC) mirrors separated by a spacer W. Arrows indicate transmission peaks related to first and second order FP resonances. Experimental spectra (black lines) are compared with 2D finite difference time-domain (FDTD) calculated spectra (gray lines). The Airy's function best-fit (gray dashed line) of the first order peak for a = 340 nm is the shown in the inset. (b) Sketch of the typical layout for 1D FP cavity. The actual cavity width W' taking into account the finite penetration depth L_p of the field inside the mirrors is shown.

While these modes are insensitive to defects and disorder, they are strongly influenced by the *modal conversion* and light propagation is affected by the single hole shape parameters (*e.g.*, the hole depth). Thus, since <z> (#2) > z (#1), inside the stopgap light transmission is lowered in sample #2 with respect to sample #1, while R and cavity Q values result to be improved.

CONCLUSIONS

We have reported on the optical properties of 2D PCs etched in InP/GaInAsP slab waveguide structures. The combination between structural analysis and optical characterization by ILS experiments makes possible to evaluate which improvements are necessary in the fabrication process. Two different regimes are identified for light propagation inside the PC structure. When light with energies outside the PBG is considered, out-of-plane losses are the limiting factor for PC performances. Improvements in the hole shape and in the ordering of the PC pattern should allow one to lower the scattering towards the substrate. On the other hand, when entering the stopgap, the hole "physical" parameters (*e.g.*, the hole depth) strongly affect the PC optical properties.

ACKNOWLEDGEMENTS

This work was supported by the European Union in the framework of the IST project PCIC (Contract n. 1999-11239).

REFERENCES

1. J.D. Joannopoulos, R.D. Meade, and J.N. Winn, *Molding the Flow of Light* (Princeton University Press, Princeton NJ, 1995).
2. E. Yablonovitch, Phys. Rev. Lett. **58**, 2059 (1987).
3. H. Benisty, C. Weisbuch, D. Labilloy, M. Rattier, C.J.M. Smith, T.F. Krauss, R.M. De La Rue, R. Houdré, U. Oesterle, and D. Cassagne, IEEE J. Lightwave Technol. **17**, 2063 (1999).
4. R. Ferrini, D. Leuenberger, M. Mulot, M. Qiu, J. Moosburger, M. Kamp, A. Forchel, S. Anand, and R. Houdré, IEEE J. Quantum Electron. , submitted.
5. J. Moosburger, M. Kamp, A. Forchel, R. Ferrini, D. Leuenberger, R. Houdré, S. Anand, and J. Berggren, Nanotechnology, submitted.
6. M. Qiu, and S. He, Phys. Rev. B **61**, 12871(2000); J. Appl. Phys. **87**, 8268 (2000); Phys. Lett. A **266**, 425 (2000); ibid., **278**, 348 (2001).
7. H. Benisty, D. Labilloy, C. Weisbuch, C.J.M. Smith, T.F. Krauss, D. Cassagne, A. Béraud, and C. Jouanin, Appl. Phys. Lett. **76**, 532 (2000).
8. H. Benisty, Ph. Lalanne, S. Olivier, M. Rattier, C. Weisbuch, C.J.M. Smith, T.F. Krauss, C. Jouanin, and D. Cassagne, Opt. Quant. Electron., to be published.
9. H. Benisty (private communication)
10. W. Bogaerts, P. Bienstman, D. Taillaert, R. Baets, and D. De Zutter, IEEE Photonic Tech. L. **13**, 565 (2001).